

Synthesis and some octahedral complexes of a chiral triaza macrocycle

Simon W. Golding,^a Trevor W. Hambley,^b Geoffrey A. Lawrance,^{*a} Stephan M. Luther,^a Marcel Maeder^a and Peter Turner^b

^a Department of Chemistry, The University of Newcastle, Callaghan 2308, Australia

^b School of Chemistry, The University of Sydney, New South Wales 2006, Australia

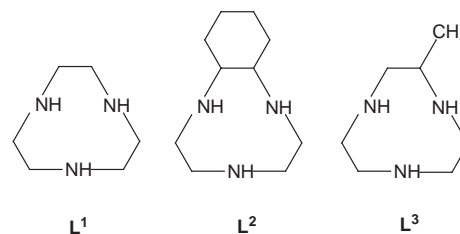
Received 23rd November 1998, Accepted 7th April 1999

The chiral and bulky tacn (1,4,7-triazacyclononane, L¹) analogue chtacn (2,5,8-triazabicyclo[7.4.0^{1,9}]tridecane, L²), which has a cyclohexane ring fused to the tacn framework, has been synthesized commencing with (±), (+)- or (-)-*trans*-cyclohexane-1,2-diamine. Syntheses and properties of cobalt(III), nickel(II), chromium(III) and iron(III) complexes are described. In the complex bis(*RR*-2,5,8-triazabicyclo[7.4.0^{1,9}]tridecane)cobalt(III) chloride hexafluorophosphate the cyclohexane rings and pairs of adjacent secondary amines occupy an approximate plane around the cobalt ion, with the remaining secondary amines in each tridentate ligand in *trans* dispositions. A large positive Cotton effect occurs under the low energy absorption band in the circular dichroism spectrum of this cobalt(III) complex of the *R,R*(-)-chtacn ligand. In the dinuclear complex aqua-di-μ-chloro-chlorobis(*SS*-2,5,8-triazabicyclo[7.4.0^{1,9}]tridecane)dinickel(II) perchlorate each nickel atom is bound to a tridentate macrocyclic ligand in different dispositions, with the distorted octahedron of each nickel completed by two bridging chloride ions and either a chloride ion or aqua molecule. For [M(Lⁿ)₂]^{m+} complexes, electronic maxima are shifted slightly to lower energy and reduction potentials slightly to more negative potential in the case of L² compared with L¹.

Introduction

The triazamacrocycle tacn (1,4,7-triazacyclononane, L¹) represents the simplest and most studied example of a cyclic polyamine capable of co-ordinating facially to an octahedral complex. First reported by Koyama and Yoshino,¹ the coordination chemistry of this molecule has been comprehensively investigated, particularly by Chaudhuri, Weighardt and co-workers.² It forms metal complexes which in all cases exceed in thermodynamic stability those of the closely related acyclic triamine 3-azapentane-1,5-diamine, an effect associated with the favourable entropy effects arising from the endodentate conformation of the tacn ligand where all ligating atoms are directed towards the macrocycle centre, diminishing rearrangement on co-ordination. Co-ordination of tacn to octahedral complexes occurs dominantly facially involving all three secondary amines; with two ligands bound, the metal ion is effectively 'sandwiched' between them. For co-ordination to square-planar metal ions, chelation by two donors only occurs, leaving one unbound but available for protonation or other interactions. The range of complexes prepared involving tacn is both extensive and diverse.²

A number of other triazamacrocycles have been prepared and aspects of their co-ordination chemistry examined. These include examples containing larger rings,^{1,3} pendants on the ring,² or incorporating aromatic units as part of the ring.⁴ Further, examples with mixed donor sets such as N₂O,^{5,6} N₂S⁷ and NS₂,⁸ as well as O₃- and S₃-tacn analogues,^{9,10} have been reported. We have been examining tetraaza macrocycles incorporating cyclohexane rings fused to the macrocycle, which introduce chirality, bulk and rigidity to the ligand system.¹¹ As an extension of this study, we are now investigating triazamacrocycles with cyclohexane rings fused to the macrocycle framework. Details of the syntheses of the analogue chtacn (2,5,8-triazabicyclo[7.4.0^{1,9}]tridecane, L²) and aspects of its co-ordination chemistry to cobalt(III), chromium(III), iron(III) and nickel(II), including crystal structure determinations of a cobalt(III) and nickel(II) complex, are reported herein.



Experimental

Syntheses

The polyamine macrocycle (L²) was prepared by a variation of the well studied Richman–Atkins procedure,^{3,12–15} as described for the successive steps below.

***N,N'*-Bis(*p*-tolylsulfonyl)-*trans*-cyclohexane-1,2-diamine.** A combination of 7.58 g (66.4 mmol) of (+)-, (-)- or (±)-*trans*-1,2-diaminocyclohexane and 5.70 g (138.2 mmol) of NaOH was dissolved in 70 cm³ water and 26.38 g (138.4 mmol) of purified *p*-toluenesulfonyl chloride dissolved in 150 cm³ of diethyl ether were added dropwise over 4 h under vigorous stirring. After addition was completed, the mixture was stirred for 45 min before 10 cm³ methanol were added. The mixture was filtered and the solid washed with water, then methanol, and recrystallised from hot methanol, giving big colourless crystals (17.7 g, 63%). NMR spectra (CDCl₃): ¹H, δ 7.75 (d, 4 H), 7.3 (d, 4 H), 4.97 (br, 2 H), 2.78 (br, 2 H), 2.4 (s, 6 H), 1.81 (br, 2 H), 1.55 (br, 2 H) and 1.11 (br, 4 H); ¹³C (¹H decoupled), δ 143.5, 137.2, 129.8, 127.3, 56.6, 33.3, 24.2 and 21.6.

***N,N*-bis[2-(*p*-tolylsulfonyloxy)ethyl]toluene-*p*-sulfonamide.**¹⁴ A mixture of 14 g (132 mmol) of diethanolamine and 130 cm³ of dry pyridine was cooled to <0 °C in an ice-salt bath. Next, 76.3 g (400.2 mmol) of purified *p*-toluenesulfonyl chloride were added in small portions so that the temperature stayed below 0 °C, and the solution was stirred for 2 h at 0 °C after completion

of the addition. Then 250 cm³ of 5 mol dm⁻³ HCl were slowly added so that the temperature always stayed <10 °C. A sticky red oil has formed and the mixture was allowed to stir overnight. The solid formed was filtered off, washed with ice-water and recrystallised from methanol (53.8 g, 72%). NMR spectra (CDCl₃): ¹H, δ 7.75 (d, 4 H), 7.6 (d, 2 H), 7.33 (d, 4 H), 7.27 (d, 2 H), 4.11 (t, 4 H), 3.37 (t, 4 H), 2.45 (s, 6 H) and 2.41 (s, 3 H); ¹³C (¹H decoupled), δ 145.2, 144.2, 135.4, 132.5, 130.1, 130.0, 128.0, 127.3, 68.3, 48.5, 21.7 and 21.5.

2,5,8-Tris(*p*-tolylsulfonyl)-2,5,8-triazabicyclo[7.4.0^{1,9}]tridecane. *N,N'*-Bis(*p*-tolylsulfonyl)-*trans*-cyclohexane-1,2-diamine (6 g, 14.2 mmol) was dissolved in 190 cm³ of dry DMF, 4.61 g (33.4 mmol) of dry K₂CO₃ were added and the mixture was heated to 50 °C for an hour. Then 9.9 g (17.4 mmol) of *N,N*-bis[2-(*p*-tolylsulfonyloxy)ethyl]toluene-*p*-sulfonamide dissolved in 100 cm³ of dry DMF were added dropwise within 26 h. The reaction mixture was kept at 50 °C for 7 d. The solution was evaporated to 50 cm³ and was poured into 2 dm³ of ice-water acidified with 10 cm³ of 10 mol dm⁻³ HCl. The precipitate was vacuum filtered, washed with ice-water and refluxed in EtOH for an hour. The solid was filtered off and dried (2.56 g, 28%).

2,5,8-Triazabicyclo[7.4.0^{1,9}]tridecane L². 2,5,8-Tris(*p*-tolylsulfonyl)-2,5,8-triazabicyclo[7.4.0^{1,9}]tridecane (2.32 g, 3.6 mmol) and dry Na₂HPO₄ (2.58 g, 18.2 mmol) were suspended in 60 cm³ of dry methanol. After addition of 3% w/w sodium amalgam (33.54 g, 43.76 mmol) the mixture was refluxed overnight. The addition of equivalent amounts of Na₂HPO₄ and sodium amalgam was repeated two times with further refluxing overnight after each addition. Water (300 cm³) was added, Hg decanted, and the solid collected and washed with water. The solution was evaporated to 100 cm³ and extracted with CH₂Cl₂ (5 × 100 cm³). The organic phase was dried over Na₂SO₄, filtered and evaporated to yield a colourless oil (0.64 g, 97%). NMR spectra (CDCl₃): ¹H, δ 2.9–2.6 (m, 8 H), 2.35 (br, 3 H), 2.25 (br, 2 H), 1.81 (br, 2 H), 1.68 (br, 2 H) and 1.19 (br, 4 H); ¹³C (¹H decoupled), δ 60.0, 46.9, 44.5, 33.9 and 26.1.

The trihydrochloride salt was prepared by dissolving the above oily product in 25 cm³ of ethanol and adding 5 cm³ of 10 mol dm⁻³ HCl. The solution was evaporated to dryness. Dry diethyl ether was added and the product collected by vacuum filtration (Found: C, 38.5; H, 8.3; N, 13.1. Calc. for C₁₀H₂₄Cl₃N₃·H₂O: C, 38.6; H, 8.4; N, 13.5%).

Metal complexes. All syntheses below were performed successfully with either racemic, *RR*- or *SS*-L², with products differing in chiroptical properties only.

Bis(2,5,8-triazabicyclo[7.4.0^{1,9}]tridecane)cobalt(III) perchlorate, [Co(L²)₂][ClO₄]₃. A solution of L²·3HCl (185 mg, 0.63 mmol) and CoCl₂·6H₂O (75 mg, 0.32 mmol) in water (50 cm³) and 1 mol dm⁻³ HCl (10 cm³) was aerated for 24 h, then activated charcoal was added and the solution refluxed for 6 h. The charcoal was filtered off and the solution diluted to 200 cm³ and loaded onto a Dowex 50W-X2 cation-exchange column (2 × 20 cm). Elution with 3 mol dm⁻³ HCl gave only two bands, a major orange and a minor red band, which were collected and evaporated to dryness. The major product was dissolved in 10 cm³ of water, the pH adjusted to 7, and 4 cm³ of 1 mol dm⁻³ NaClO₄ were added. The solution was allowed to stand for crystallisation. The orange crystals of the major band were collected, washed with cold ethanol and diethyl ether and dried (193 mg, 84%) (Found: C, 32.6; H, 5.7; N, 10.9. Calc. for C₂₀H₄₂Cl₃CoN₆O₁₂·H₂O: C, 32.4; H, 6.0; N, 11.3%). Electronic spectrum (water): λ_{max} 336 (96) and 469 nm (ε 97 dm³ mol⁻¹ cm⁻¹). NMR spectra (D₂O): ¹H, δ 3.49 (br, 2 H), 3.38–2.76 (br, 18 H), 2.38 (br, 2 H), 2.08 (br, 2 H), 1.79 (br, 8 H) and 1.26 (br, 4 H); ¹³C (¹H decoupled), δ 69.2, 64.1, 56.2, 53.9, 50.9, 44.5, 32.0, 31.5, 26.9 and 26.0. The perchlorate salt did not produce

crystals suitable for X-ray crystallography, but good quality crystals were obtained for the *RR* isomer by rotary evaporation of the yellow band obtained from column chromatography to dryness and recrystallisation of this chloride salt from water in the presence of an excess of sodium hexafluorophosphate, which yielded crystals of formula [Co(*RR*-L²)₂][PF₆]₂·2.5H₂O. The minor product did not crystallise, but was assigned as trichloro(2,5,8-triazabicyclo[7.4.0^{1,9}]tridecane)cobalt(III) by spectroscopy. Electronic spectrum (water): λ_{max} 393 and 568 nm. NMR spectra (D₂O–water): ¹³C (¹H decoupled), δ 60.1, 45.7, 42.7, 32.1 and 26.5.

Aquachloro-di-μ-chloro-bis(2,5,8-triazabicyclo[7.4.0^{1,9}]tridecane)dinickel(II) perchlorate, [Ni₂(L²)₂Cl₃(OH₂)₂][ClO₄]. A mixture of L² (486 mg, 2.65 mmol) and NiCl₂·6H₂O (630 mg, 2.65 mmol) was dissolved in ethanol (50 cm³), 1 mol dm⁻³ NaClO₄ (5 cm³) was added and the solution was allowed to stand for crystallisation. Blue crystals formed and were collected, washed with cold ethanol and recrystallised from water (0.96 g, 52%) (Found: C, 33.75; H, 6.3; N, 11.6. Calc. for C₂₀H₄₄Cl₄N₆Ni₂O₅: C, 33.9; H, 6.3; N, 11.85%). Electronic spectrum (water): λ_{max} 352 (18), 433 (sh), 575 (10) and 780 nm (ε 6 dm³ mol⁻¹ cm⁻¹). Crystals employed for X-ray crystallography contained SS-L².

Bis(2,5,8-triazabicyclo[7.4.0^{1,9}]tridecane)nickel(II) nitrate, [Ni(L²)₂][NO₃]₂. Compound L² (425 mg, 2.32 mmol) and Ni(NO₃)₂·6H₂O (337 mg, 1.16 mmol) were dissolved in water (75 cm³). The pH was adjusted to 8 with NaOH, and the solution set aside to crystallise. The pink crystalline product formed was collected, washed with cold ethanol and recrystallised from water (0.26 g, 45%) (Found: C, 43.65; H, 7.8; N, 20.8. Calc. for C₂₀H₄₂N₈NiO₆: C, 43.7; H, 7.7; N, 20.4%). Electronic spectrum (water): λ_{max} 290 (23), 508 (7) and 812 (ε 9 dm³ mol⁻¹ cm⁻¹) and 880 (sh) nm.

Bis(2,5,8-triazabicyclo[7.4.0^{1,9}]tridecane)chromium(III) chloride perchlorate pentahydrate, [Cr(L²)₂Cl₂][ClO₄]₂·5H₂O. The compound CrCl₃·6H₂O (727 mg, 2.73 mmol) was dissolved in DMSO (40 cm³) at 190 °C and the solution evaporated to 25 cm³. The solution was cooled to 70 °C and 1 g (5.45 mmol) of L² in 10 cm³ ethanol was added. The temperature was raised to 170 °C and the DMSO completely evaporated. The product was dissolved in water, diluted to 500 cm³ and loaded onto a Dowex 50W-X2 cation-exchange column (3 × 25 cm). After washing with 1 mol dm⁻³ HCl to remove unco-ordinated Cr^{III}, first a red and then a major orange second band were eluted with 4 mol dm⁻³ HCl. The volume was reduced to 15 cm³, solid NaClO₄ was added and the solution set aside to crystallise (226 mg, 15%; further crops on extended standing) (Found: C, 35.6; H, 7.8; N, 12.1. Calc. for C₂₀H₅₂Cl₃CrN₆O₉: C, 35.4; H, 7.7; N, 12.35%). Electronic spectrum (water): λ_{max} 345 (55) and 446 nm (ε 83 dm³ mol⁻¹ cm⁻¹).

Bis(2,5,8-triazabicyclo[7.4.0^{1,9}]tridecane)iron(III) chloride hexahydrate, [Fe(L²)₂Cl₃·6H₂O]. The compound FeCl₃·6H₂O (740 mg, 2.73 mmol) was dissolved in DMSO (30 cm³) at 140 °C, the resultant solution cooled to 25 °C, L² (1 g, 5.45 mmol) in ethanol (10 cm³) added with stirring and the temperature raised to 150 °C. The solution was evaporated to 10 cm³ and the yellow-brown precipitate collected. The product was washed with cold ethanol and recrystallised from water. Orange crystals were collected, washed with ethanol and diethyl ether and air dried (413 mg, 29%) (Found: C, 37.2; H, 8.3; N, 12.7. Calc. for C₂₀H₄₂Cl₃FeN₆·6H₂O: C, 37.7; H, 8.5; N, 13.2%). Electronic spectrum (water): λ_{max} 347 (281), 435 (ε 73 dm³ mol⁻¹ cm⁻¹) and 512 (sh) nm.

Spectroscopic methods

Absorption spectra were recorded using a Hitachi 150-20 spectrophotometer and circular dichroism spectra using a JASCO J-710 spectropolarimeter operating with J-700 Windows software, employing aqueous solutions. Infrared

spectra were recorded on a Bio-Rad FTS-7 FT-IR spectrometer for compounds dispersed in KBr discs, and NMR spectra on a Bruker Avance DPX300 spectrometer in either CDCl₃ solution (for ligands) or D₂O (for complexes). Voltammetry in aqueous solution (with 0.1 mol dm⁻³ sodium perchlorate as electrolyte) employed a conventional three-electrode system and nitrogen purge gas, using a BAS Model CV-27 electrochemical controller. A glassy carbon working electrode polished with alumina before measurement of each voltammogram, a Ag–AgCl reference electrode and a platinum wire auxiliary electrode were used. The potentials reported were converted into those referred to the normal hydrogen electrode (NHE). The scan rate for cyclic voltammetry results reported was usually 100 mV s⁻¹. Microanalyses were performed by the Research School of Chemistry Microanalytical Service at the Australian National University.

X-Ray crystallography

Cell constants were determined by least-squares fits to the setting parameters of 25 independent reflections, measured and refined on a Rigaku AFC7R diffractometer, [Ni₂(SS-L²)₂-Cl₃(OH₂)] [ClO₄] **A**, or an Enraf-Nonius CAD4-F diffractometer [Co(RR-L²)₂][PF₆]₂Cl·2.5H₂O **B**, employing graphite monochromated Cu-Kα radiation (1.5418 Å) for **A** and Mo-Kα (0.71069 Å) for **B**. Data reduction and application of Lorentz-polarisation and ψ scan and analytical absorption corrections (**A** and **B** respectively) were carried out using TEXSAN.¹⁶ The structures were solved by direct methods using SHELXS 86¹⁷ and refined using full-matrix least-squares methods with TEXSAN.¹⁶ Hydrogen atoms were included at calculated sites with thermal parameters derived from the parent atoms. The hydrogen atoms of one of the co-ordinated water molecules of **A** were located in the difference map and included at these sites without further refinement. Non-hydrogen atoms were refined anisotropically. Scattering factors and anomalous dispersion terms for Ni and Co (neutral atoms) were taken from ref. 18. Anomalous dispersion effects were included in F_c ; the values for $\Delta f'$ and $\Delta f''$ were those of Creagh and McAuley.²⁰ The values for the mass attenuation coefficients are those of Creagh and Hubbell.²¹ All other calculations were performed using TEXSAN.¹⁶ Selected bond lengths and angles are listed in Tables 2 and 3. The atomic nomenclature is defined in Figs. 2 and 3.²²

Crystal data. [Ni₂(SS-L²)₂Cl₃(OH₂)] [ClO₄], C₂₀H₄₄Cl₄N₆Ni₂O₅, $M = 707.80$, monoclinic, space group $P2_1$, $a = 14.406(3)$, $b = 7.845(1)$, $c = 26.639(41)$ Å, $\beta = 102.60(1)^\circ$, $U = 2938(1)$ Å³, D_c ($Z = 4$) = 1.600 Mg m⁻³, $\mu(\text{Cu-K}\alpha) = 3.069$ mm⁻¹, $F(000) = 1480$, $T = 294$ K. Specimen: purple needles; $N = 4953$, $N_o = 3996$ [$|F_o| > 2.5\sigma(|F_o|)$, $38 < \theta < 61^\circ$], hkl 0 to 16, 0 to 8, -29 to 29. Final $R = 0.0426$, $R' = 0.0475$, parameters = 665, goodness of fit = 2.420. Residual extrema +0.49, -0.56 e Å⁻³.

[Co(RR-L²)₂][PF₆]₂Cl·2.5H₂O, C₂₀H₄₇ClCoF₁₂N₆O_{2.5}P₂, $M = 795.94$, monoclinic, space group $C2$, $a = 20.443(2)$, $b = 9.994(2)$, $c = 8.8967(7)$ Å, $\beta = 112.78(1)^\circ$, $U = 1682.1(4)$ Å³, D_c ($Z = 2$) = 1.577 Mg m⁻³, $\mu(\text{Mo-K}\alpha) = 0.782$ mm⁻¹, $F(000) = 882$, $T = 294$ K. Specimen: orange needles; $N = 1585$, $N_o = 1485$ [$|F_o| > 2.5\sigma(|F_o|)$, $2 < \theta < 25^\circ$], hkl -24 to 22, 0 to 11, 0 to 10. Final $R = 0.0526$, $R' = 0.0534$, parameters = 202, goodness of fit = 4.442. Residual extrema +0.62, -0.40 e Å⁻³.

CCDC reference number 186/1416.

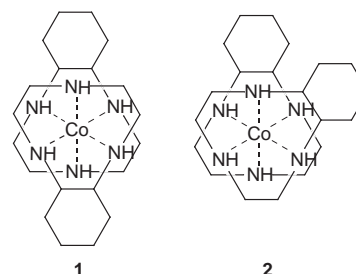
See <http://www.rsc.org/suppdata/dt/1999/1975/> for crystallographic files in .cif format.

Results and discussion

The molecule L², as a triazamacrocycle with a nine-membered saturated ring, is a close analogue of the well known L^{1,2} but with one of the CH₂CH₂ links between two secondary amine

groups replaced by a cyclohexane unit. This is achieved by commencing with tosylated *trans*-cyclohexane-1,2-diamine and reacting with tosylated diethanolamine in a Richman–Atkins procedure, a process which yields the target small ring macrocycle with a reasonable yield of approximately 30%. An alternative procedure of treating dibromocyclohexane with a tritosylated triamine was not successful. Failure of this particular route can be interpreted in terms of steric hindrance of the initial substitution step, similar to arguments proposed earlier for a bulky nucleophile attacking a sterically hindered site.¹⁵ Steric hindrance is reduced in the successful method developed here, but the yield remains lower than achieved for the less bulky tacn. The free amine is obtained from the tosylated intermediate by employing sodium amalgam as the detosylating agent, a highly efficient reaction where the triamine is recovered in essentially stoichiometric yield provided a large amount of freshly prepared amalgam is employed. Spectroscopy is consistent with the formulation of the product as L²; for example, five resonances are detected in the methylene region of the proton-decoupled ¹³C NMR spectrum, as required. Confirmation of the structure comes in the structural studies reported later. The potentially tridentate ligand L² possesses two chiral carbon centres, and resolution of the precursor diamine prior to macrocycle synthesis yields an optically active macrocycle, since the chiral centres are not involved in any of the chemistry. In addition, the cyclohexane ring fused to the ring framework provides both a bulkier and more rigid macrocycle. As expected, the co-ordination chemistry (apart from chiroptical properties) of the racemic, *RR*- or *SS*-L² forms is identical, and hence in discussion below reference to a particular optical isomer is made only when discussing circular dichroism spectroscopy.

Octahedral complexes of cobalt(III), chromium(III), iron(III) and nickel(II) with two L² molecules co-ordinated as tridentate ligands to two opposite octahedral faces have been prepared. The octahedral cobalt(III) complex has been characterised by a crystal structure analysis, and may represent the common isomer met in the series, although this awaits further structural studies. No great difficulty in preparing the bis(triamine) complexes was encountered, although it is known that some triazamacrocycles form only 1:1 complexes.² In addition to the 1:2 nickel(II) complex, a dinuclear nickel(II) complex where a single L² is co-ordinated to each of two nickel(II) ions was isolated and characterised by a crystal structure analysis. Again, tridentate co-ordination of the macrocycle is observed. There is no evidence to suggest that the 1:1 complex is preferred, the dinuclear mono and mononuclear bis complexes arising from slightly different syntheses. The bis(L²) metal complexes can in principle exist in two geometric isomers (**1** and **2** below). We did not detect in the chromatographic isolation of complexes more than one band assignable to bis(L²) species, with any minor additional band characteristic of a mono(L²) complex. This may mean that only one isomer is formed following equilibration, or else that separation is not readily achieved. However, at least for the diamagnetic cobalt(III) complex, NMR spectroscopy of the crude evaporated band off the column does not show multiple sets of resonances, indicative of dominantly one isomer (**1**).



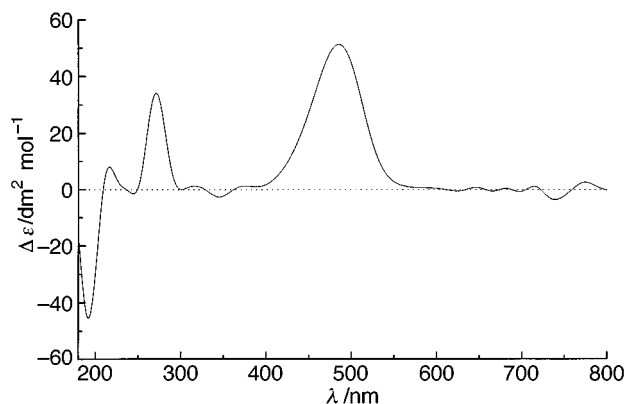


Fig. 1 Circular dichroism spectrum of $[\text{Co}(\text{RR-L}^2)](\text{ClO}_4)_3$.

Table 1 Comparison of the electronic spectra and redox potentials of $[\text{M}(\text{L}^1)_2]^{n+}$ and $[\text{M}(\text{L}^2)_2]^{n+}$ complexes

M^{n+}	Ligand	$\lambda_{\text{max}}/\text{nm}$ ($\epsilon_{\text{max}}/\text{dm}^3 \text{ mol}^{-1} \text{ cm}^{-1}$)	$E_{1/2}/\text{V}$ vs. NHE
Co^{III}	L^1	333 (89), 458 (100)	-0.41
	L^2	336 (96), 469 (97)	-0.46
Cr^{III}	L^1	340 (64), 439 (88)	-1.14
	L^2	345 (55), 446 (83)	-1.21
Fe^{III}	L^1	336 (288), 430 (82), 500 (sh)	+0.13
	L^2	347 (281), 435 (73), 512 (sh)	+0.03
Ni^{II}	L^1	308 (12), 505 (5), 800 (7), 870 (sh)	+0.95
	L^2	290 (23), 508 (7), 812 (9), 880 (sh)	+0.86

Previously, the only substituted chiral analogue of tacn reported was the *R*-2-methyl-1,4,7-triazacyclononane (L^3).²³ Examination of this system arose following the observation that crystals of the unsubstituted $[\text{Co}(\text{L}^1)_2]\text{Cl}_3$ spontaneously resolve on crystallising, the individual chelate rings in a bound ligand having a preferred common configuration $\lambda\lambda\lambda$ (or $\delta\delta\delta$). Optical activity cannot arise as a result of disposition of the ligands in this system, but solely from the dissymmetric chelate ring conformations, producing a relatively large Cotton effect. With *R-L*³, the largest ring-conformation optical activity reported was observed. Unfortunately, X-ray crystallography showed orientational disorder of the methyl group,²⁴ and nine geometrical and configurational isomers are possible, partly separated by chromatography on SP-Sephadex.²⁵

Oriental disorder is removed and the number of possible isomers is reduced in the present study with L^2 . The CD of the cobalt(III) complex of the *R,R*(-) isomer of L^2 is dominated by a very strong Cotton effect under the lowest energy transition at 486 nm of $\Delta\epsilon + 51.4 \text{ dm}^2 \text{ mol}^{-1}$ (Fig. 1). The maximum lies to lower energy than the absorption maximum (469 nm), and is most likely associated with the low-energy ${}^1\text{A}_1 \rightarrow {}^1\text{E}$ component under the ${}^1\text{A}_1\text{g} \rightarrow {}^1\text{T}_{1\text{g}}$ octahedral transition envelope, similar to the behaviour for $[\text{Co}(\text{nn})_3]^{3+}$ complexes (nn = ethane-1,2-diamine, *R*-propane-1,2-diamine or *R,R*-cyclohexane-1,2-diamine).²⁶ For these and related complexes a positive Cotton effect is associated with the *D* absolute configuration of the complex. Whereas the distribution of chelate rings is an important component in these tris(bidentate ligand) systems, in the L^2 complex the large Cotton effect arises chiefly from the dissymmetric chelate ring conformations. The $\delta\delta\delta$ conformations in the L^2 complex produce the same sign of Cotton effect under the low energy d-d transition as the $\delta\delta\delta$ conformations in L^3 , with the size of the transition larger (by ca. 20%) for the L^2 complex. A much less intense set of bands occurs under the higher energy ${}^1\text{A}_1\text{g} \rightarrow {}^1\text{T}_{2\text{g}}$ octahedral transition envelope, with additional strong Cotton effects between 180 and 300 nm presumably associated with charge transfer transitions and $n \rightarrow \pi^*$ transitions of the ligand.

A comparison of the electronic spectra and metal-centred redox properties of bis(triamine)metal complexes of L^1 and L^2 appears in Table 1. It is immediately noticeable that, in all cases,

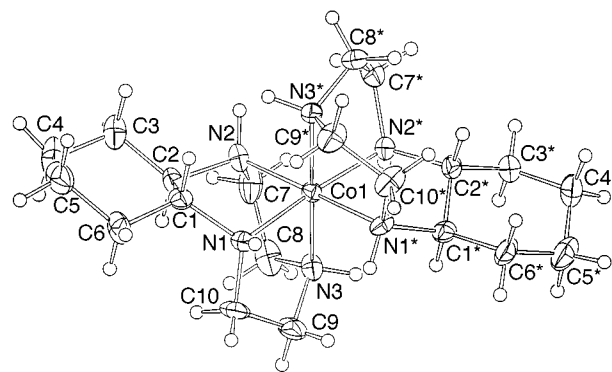


Fig. 2 A view of the $[\text{Co}(\text{RR-L}^2)]^{3+}$ cation, including atom numbering.

Table 2 Selected bond distances (\AA) and angles ($^\circ$) for $[\text{Co}(\text{RR-L}^2)]^{3+}$

$\text{Co}(1)-\text{N}(1)$	1.976(7)	$\text{Co}(1)-\text{N}(1^*)$	1.977(7)
$\text{Co}(1)-\text{N}(2)$	1.976(8)	$\text{Co}(1)-\text{N}(2^*)$	1.975(8)
$\text{Co}(1)-\text{N}(3)$	1.948(5)	$\text{Co}(1)-\text{N}(3^*)$	1.948(5)
$\text{N}(1)-\text{Co}(1)-\text{N}(1^*)$	92.4(4)	$\text{N}(1)-\text{Co}(1)-\text{N}(2)$	84.8(2)
$\text{N}(1)-\text{Co}(1)-\text{N}(2^*)$	176.0(4)	$\text{N}(1)-\text{Co}(1)-\text{N}(3)$	85.3(3)
$\text{N}(1)-\text{Co}(1)-\text{N}(3^*)$	97.4(3)	$\text{N}(1^*)-\text{Co}(1)-\text{N}(2)$	176.0(4)
$\text{N}(1^*)-\text{Co}(1)-\text{N}(2^*)$	84.8(2)	$\text{N}(1^*)-\text{Co}(1)-\text{N}(3)$	97.4(3)
$\text{N}(1^*)-\text{Co}(1)-\text{N}(3^*)$	85.3(3)	$\text{N}(2)-\text{Co}(1)-\text{N}(2^*)$	98.1(4)
$\text{N}(2)-\text{Co}(1)-\text{N}(3)$	85.2(4)	$\text{N}(2)-\text{Co}(1)-\text{N}(3^*)$	92.3(3)
$\text{N}(2^*)-\text{Co}(1)-\text{N}(3)$	92.3(3)	$\text{N}(2^*)-\text{Co}(1)-\text{N}(3^*)$	85.1(4)
$\text{N}(3)-\text{Co}(1)-\text{N}(3^*)$	176.1(7)		

maxima for the L^2 complexes are shifted to slightly lower energy than those for the L^1 complex, indicative of a slightly weaker ligand field for the new ligand L^2 compared with L^1 . Calculation of $10Dq$ for L^2 from spectroscopy of the nickel(II) compounds yields ca. $12\,300 \text{ cm}^{-1}$ compared with a value of ca. $12\,500 \text{ cm}^{-1}$ reported for L^1 .²⁷ The origins of this small difference are presumably steric, related to the bulk of the cyclohexane ring fused to the macrocycle ring adjacent to two of the nitrogen donors. Although there is no required relationship between redox potentials and electronic maxima, it is also notable that a reasonably consistent shift in redox potentials from L^1 to L^2 also occurs (Table 1). All four $[\text{M}(\text{L}^2)_2]^{n+}$ complexes display reversible or quasireversible couples in the cyclic voltammetry (50 mV s^{-1} scan rate, glassy carbon working electrode, aqueous $0.1 \text{ mol dm}^{-3} \text{ NaClO}_4$) varying in potential from +0.86 V (ΔE 90 mV) for the $\text{Ni}^{\text{III/II}}$ couple, +0.03 V (ΔE 74 mV) for $\text{Fe}^{\text{III/II}}$, -0.46 V (ΔE 76 mV) for $\text{Co}^{\text{III/II}}$, and to -1.21 V (ΔE 90 mV) for $\text{Cr}^{\text{III/II}}$, cited *versus* the NHE. These range from 50 to 100 mV more negative than the values reported for the corresponding compound in the $[\text{M}(\text{L}^1)_2]^{n+}$ series.

The $[\text{Co}(\text{RR-L}^2)](\text{PF}_6)_2\text{Cl}\cdot 2.5\text{H}_2\text{O}$ complex crystallised in the $C2$ space group. The structure (Fig. 2) consists of a complex cation located on a crystallographic twofold rotation axis, a chloride anion also on a twofold rotation axis, a hexafluorophosphate anion and two water molecules, one at a general site and the other on a twofold rotation axis. The complex cation displays a distorted octahedral geometry and has the cyclohexane groups located *trans* to one another. There are no obvious steric reasons for this arrangement being preferred. As with the nickel complex discussed below, bond lengths and angles are not abnormal, although the $\text{Co}-\text{N}(3)$ bond [1.948(5) \AA] is significantly shorter than the two $\text{Co}-\text{N}$ bond adjacent to the cyclohexane ring [$\text{Co}-\text{N}(1)$ 1.976(7), $\text{Co}-\text{N}(2)$ 1.976(8) \AA] and is at the short end of the range for hexaminecobalt(III) systems. With the two longer bonds associated with the two secondary nitrogen atoms adjacent to the cyclohexane ring, it is tempting to assign the elongation to steric effects. However, the longer and not the shorter distances are very similar to the average distance reported for $[\text{Co}(\text{L}^3)_2]^{3+}$ of 1.974 \AA ,²⁴ which suggests that steric influences of the cyclohexane ring are not marked.

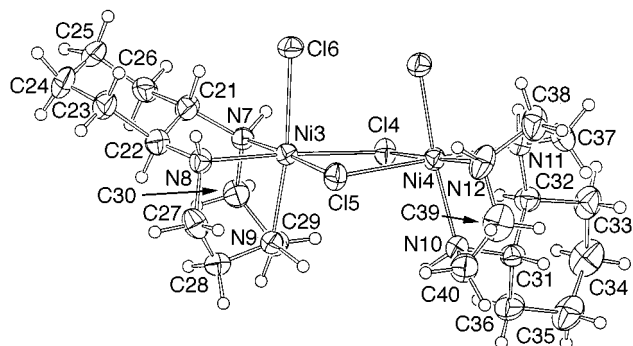


Fig. 3 A view of the $[\text{Ni}_2(\text{SS-L}^2)_2\text{Cl}_3(\text{OH}_2)]^+$ cation, including atom numbering.

Table 3 Selected bond distances (Å) and angles (°) for $[\text{Ni}_2(\text{SS-L}^2)_2\text{Cl}_3(\text{OH}_2)]^+$

Ni(1)–Cl(1)	2.471(3)	Ni(1)–Cl(2)	2.404(2)
Ni(1)–Cl(3)	2.480(2)	Ni(1)–N(1)	2.081(7)
Ni(1)–N(2)	2.060(9)	Ni(1)–N(3)	2.075(8)
Ni(2)–Cl(1)	2.460(2)	Ni(2)–Cl(2)	2.421(3)
Ni(2)–O(1)	2.169(5)	Ni(2)–N(4)	2.080(7)
Ni(2)–N(5)	2.056(7)	Ni(2)–N(6)	2.07(1)
Ni(3)–Cl(4)	2.381(2)	Ni(3)–Cl(5)	2.518(3)
Ni(3)–Cl(6)	2.454(2)	Ni(3)–N(7)	2.103(9)
Ni(3)–N(8)	2.081(7)	Ni(3)–N(9)	2.074(7)
Ni(4)–Cl(4)	2.442(3)	Ni(4)–Cl(5)	2.444(2)
Ni(4)–O(2)	2.151(6)	Ni(4)–N(10)	2.054(7)
Ni(4)–N(11)	2.087(7)	Ni(4)–N(12)	2.06(1)
Cl(1)–Ni(1)–Cl(2)	85.62(9)	Cl(1)–Ni(1)–Cl(3)	90.72(9)
Cl(1)–Ni(1)–N(1)	98.0(3)	Cl(1)–Ni(1)–N(2)	174.7(2)
Cl(1)–Ni(1)–N(3)	91.8(3)	Cl(2)–Ni(1)–Cl(3)	90.03(8)
Cl(2)–Ni(1)–N(1)	176.4(3)	Cl(2)–Ni(1)–N(2)	94.1(2)
Cl(2)–Ni(1)–N(3)	97.1(2)	Cl(3)–Ni(1)–N(1)	90.0(2)
Cl(3)–Ni(1)–N(2)	94.6(2)	Cl(3)–Ni(1)–N(3)	172.6(2)
N(1)–Ni(1)–N(2)	82.3(3)	N(1)–Ni(1)–N(3)	82.8(3)
N(2)–Ni(1)–N(3)	83.0(3)	Cl(1)–Ni(2)–Cl(2)	85.50(9)
Cl(1)–Ni(2)–O(1)	87.3(2)	Cl(1)–Ni(2)–N(4)	100.4(2)
Cl(1)–Ni(2)–N(5)	174.6(3)	Cl(1)–Ni(2)–N(6)	92.6(3)
Cl(2)–Ni(2)–O(1)	88.0(2)	Cl(2)–Ni(2)–N(4)	92.0(3)
Cl(2)–Ni(2)–N(5)	99.4(3)	Cl(2)–Ni(2)–N(6)	174.8(3)
O(1)–Ni(2)–N(4)	172.2(3)	O(1)–Ni(2)–N(5)	90.5(2)
O(1)–Ni(2)–N(6)	96.7(4)	N(4)–Ni(2)–N(5)	81.9(3)
N(4)–Ni(2)–N(6)	83.6(4)	N(5)–Ni(2)–N(6)	82.7(3)
Cl(4)–Ni(3)–Cl(5)	85.84(9)	Cl(4)–Ni(3)–Cl(6)	91.56(9)
Cl(4)–Ni(3)–N(7)	96.3(2)	Cl(4)–Ni(3)–N(8)	176.4(2)
Cl(4)–Ni(3)–N(9)	94.4(2)	Cl(5)–Ni(3)–Cl(6)	89.1(1)
Cl(5)–Ni(3)–N(7)	177.0(2)	Cl(5)–Ni(3)–N(8)	94.8(2)
Cl(5)–Ni(3)–N(9)	95.6(3)	Cl(6)–Ni(3)–N(7)	93.0(2)
Cl(6)–Ni(3)–N(8)	92.0(2)	Cl(6)–Ni(3)–N(9)	172.6(2)
N(7)–Ni(3)–N(8)	83.0(3)	N(7)–Ni(3)–N(9)	82.1(3)
N(8)–Ni(3)–N(9)	81.9(3)	Cl(4)–Ni(4)–Cl(5)	86.16(9)
Cl(4)–Ni(4)–O(2)	89.1(2)	Cl(4)–Ni(4)–N(10)	96.4(3)
Cl(4)–Ni(4)–N(11)	93.7(3)	Cl(4)–Ni(4)–N(12)	175.4(3)
Cl(5)–Ni(4)–O(2)	88.4(2)	Cl(5)–Ni(4)–N(10)	95.4(2)
Cl(5)–Ni(4)–N(11)	179.2(2)	Cl(5)–Ni(4)–N(12)	98.4(2)
O(2)–Ni(4)–N(10)	173.6(3)	O(2)–Ni(4)–N(11)	92.4(2)
O(2)–Ni(4)–N(12)	90.4(3)	N(10)–Ni(4)–N(11)	83.9(3)
N(10)–Ni(4)–N(12)	83.9(4)	N(11)–Ni(4)–N(12)	81.8(3)
Ni(1)–Cl(1)–Ni(2)	92.7(1)	Ni(1)–Cl(2)–Ni(2)	95.3(1)
Ni(3)–Cl(4)–Ni(4)	95.2(1)	Ni(3)–Cl(5)–Ni(4)	91.7(1)

The contraction of the additional bond resembles the contraction observed with C-pendant macrocycles, such as in (*trans*-6,13-dimethyl-1,4,8,11-tetraazacyclotetradecane-6,13-diamine)cobalt(III), where the bond distance to the pendant amine is significantly reduced compared to the other two, a result of steric demands of the ligand in that case.²⁸ However, there are in the present case no unique deformations around N(3) and adjacent atoms which distinguish it from N(1) and N(2), and the close approach may simply reflect the absence of constraining cyclohexane rings on the carbon chains joined to N(3).

The structure (Fig. 3) of the dinickel(II) complex of SS-L² consists of two independent dimeric complex cations and two perchlorate anions. Tridentate co-ordination of the ligand L² is confirmed. The dimers consist of two Ni(L²) units bridged by two μ -chloro ligands. The co-ordination sphere of one of the Ni atoms is completed by a chloro ligand and the other by an aqua ligand with an intramolecular hydrogen bond [O(1)···Cl(3) 3.316(7), O(2)···Cl(6) 3.347 Å] between these two ligands producing a bend in the Ni₂Cl₂ plane. Additional asymmetry in the dimers arises from the orientation of the L² ligand. In both of the independent molecules one ligand has the cyclohexane ring lying in the Ni₂Cl₂ plane and the other ligand has it lying perpendicular to this plane. It is not clear whether this is a consequence of the difference in the nature of the axial ligands but there are no obvious steric reasons for the difference. It is possible that a number of isomers form in solution and this is the one that crystallises preferentially; the solution is very likely a complex mixture, as the bis(triamine)nickel(II) ions also crystallise from a similar reaction solution. The two independent molecular cations have the same arrangement of the tridentate ligands but are diastereomers. It is also not clear why the complex forms with one axial chloro ligand and one axial aqua ligand. However, if both axial ligands were chlorides the repulsion between them would lead to a folding in the opposite direction and a consequent repulsion between the amine ligands. Bond lengths and angles about the Ni are normal for amine complexes of this type and do not indicate that co-ordination of the tridentate ligand is accompanied by the induction of significant stress.

The presence of a cyclohexane ring fused onto the basic tacn framework clearly influences the co-ordination chemistry involving this ligand somewhat. Nevertheless, the ability of a relatively rigid chiral tacn ligand to form 1:2 complexes with octahedral metal ions has been established, and aspects of the co-ordination chemistry of these described. We are extending our studies to examine the effect of increasing the number of fused rings around the tacn core.

Acknowledgements

Support of the Australian Research Council for this project is gratefully acknowledged.

References

- H. Koyama and T. Yoshino, *Bull. Chem. Soc. Jpn.*, 1972, **45**, 481.
- P. Chaudhuri and K. Wieghardt, *Prog. Inorg. Chem.*, 1987, **35**, 329 and refs. therein.
- J. E. Richman and T. J. Atkins, *J. Am. Chem. Soc.*, 1974, **96**, 2268.
- L. T. Taylor and D. H. Busch, *J. Am. Chem. Soc.*, 1967, **89**, 5372.
- W. Rasshofer, W. Wehner and F. Vögtle, *Liebigs Ann. Chem.*, 1976, 916.
- R. D. Hancock and V. J. Thöm, *J. Am. Chem. Soc.*, 1982, **104**, 291.
- A. McAuley and S. Subramanian, *Inorg. Chem.*, 1990, **29**, 2830.
- L. R. Gahan, G. A. Lawrance and A. M. Sargeson, *Aust. J. Chem.*, 1982, **35**, 1119.
- D. Parker, *Macrocyclic Synthesis: A Practical Approach*, Oxford University Press, 1996.
- L. A. Ochrymowycz, D. Gerber, P. Chongsawangvirod and A. K. Leung, *J. Org. Chem.*, 1977, **42**, 2644.
- P. V. Bernhardt, B. Elliott, G. A. Lawrance, M. Maeder, M. A. O'Leary, G. Wei and E. N. Wilkes, *Aust. J. Chem.*, 1994, **47**, 1771.
- T. J. Atkins, J. E. Richman and W. F. Oettle, *Org. Synth.*, 1979, **58**, 86.
- F. Chavez and A. D. Sherry, *J. Org. Chem.*, 1989, **54**, 2290.
- G. H. Searle and R. J. Geue, *Aust. J. Chem.*, 1984, **37**, 959.
- P. G. Graham and D. C. Weatherburn, *Aust. J. Chem.*, 1983, **36**, 2349.
- TEXSAN, Crystal Structure Analysis Package, Molecular Structure Corporation, The Woodlands, TX, 1985 and 1992.
- G. M. Sheldrick, SHELXS 86, in *Crystallographic Computing 3*, eds. G. M. Sheldrick, C. Krüger and R. Goddard, Oxford University Press, pp. 175–189.
- D. T. Cromer and J. T. Waber, *International Tables for X-Ray Crystallography*, Kynoch Press, Birmingham, 1974, vol. IV.

- 19 J. A. Ibers and W. C. Hamilton, *Acta Crystallogr.*, 1964, **17**, 781.
- 20 D. C. Creagh and W. J. McAuley, *International Tables for Crystallography*, ed. A. J. C. Wilson, Kluwer, Boston, 1992, vol. C, Table 4.2.6.8, pp. 219–222.
- 21 D. C. Creagh and J. H. Hubbell, *International Tables for Crystallography*, ed. A. J. C. Wilson, Kluwer, Boston, 1992, vol. C, Table 4.2.4.3, pp. 200–206.
- 22 C. K. Johnson, ORTEP, A Thermal Ellipsoid Plotting Program, Oak Ridge National Laboratory, Oak Ridge, TN, 1965.
- 23 S. F. Mason and R. D. Peacock, *Inorg. Chim. Acta*, 1976, **19**, 75.
- 24 M. Mikami, R. Kuroda, M. Konno and Y. Saito, *Acta Crystallogr., Sect. B*, 1977, **33**, 1485.
- 25 M. Nonoyama, *Inorg. Chim. Acta*, 1978, **9**, 211.
- 26 C. F. Hawkins, *Absolute Configuration of Metal Complexes*, Wiley-Interscience, New York, 1971, ch. 5.
- 27 S. M. Hart, J. C. A. Boeyens and R. D. Hancock, *Inorg. Chem.*, 1983, **22**, 982.
- 28 P. V. Bernhardt, G. A. Lawrance and T. W. Hambley, *J. Chem. Soc., Dalton Trans.*, 1989, 1059.

Paper 8/09125K